



## Dynamics of extremely anisotropic etching of InP nanowires by HCl

Magnus T. Borgström<sup>\*</sup>, Jesper Wallentin, Kenichi Kawaguchi<sup>1</sup>, Lars Samuelson, Knut Deppert

Solid State Physics, Lund University, Box 118, S-22100 Lund, Sweden

### ARTICLE INFO

#### Article history:

Received 9 November 2010

In final form 20 December 2010

Available online 23 December 2010

### ABSTRACT

We report on the dynamics of *in situ* etching of nanowires using an etching agent which allows for parameter optimization for nanowire synthesis without concerns of tapering issues. Upon etching of InP nanowires using HCl it is found that HCl mainly reacts with the precursor TMI, its decomposition species, and physisorbed In. The reaction with solid InP is less rapid and diffusion limited. We find a gas-phase etch process which is metal assisted and has a high aspect ratio of 1:100.

© 2011 Elsevier B.V. All rights reserved.

### 1. Introduction

Semiconductor nanowires [1–3] (NWs) have emerged as promising building blocks for nanoelectronics [4], offering to integrate high performance III–V materials with silicon [5]. A great challenge is to create NWs with high purity, and which are uniform in length and diameter. We have recently shown that *in situ* etching allows for total control over axial and radial NW growth rates [6]. This allows to optimize a number of parameters for NW synthesis such as growth rate [7], temperature [8–10], and input V/III ratio [9–11], without concerns of tapering. We report the dynamics of *in situ* InP NW etching by use of hydrogen chloride (HCl) **after** growth, and compare the results to those obtained **during** growth [6]. A gas-phase metal assisted etch process is found with a high aspect ratio of 1:100. Etching of nanostructures in a metalorganic vapor-phase epitaxy (MOVPE) system allows temperature and concentration dependent studies over a wider parameter range as compared to metal-assisted wet etching [12]. We have previously identified three mechanisms that could result in constant NW diameter over a defined HCl parameter space for etching **during** growth [6]: (1) selectivity of the process due to the original NW side facets having a lower surface free energy than those formed during sidewall growth (2) desorption of InCl from the NW side facets being rate limiting [13]. (3) Indium species physisorbed on the side facets being more vulnerable to Cl attack, as compared to chemisorbed In situated within the core of the NW formed during axial growth. In the following, we will falsify two and indicate the most probable of the proposed hypothesis by etch experiments **after** growth where only chemisorbed species, and In dissolved in the Au particle are involved in the reaction.

### 2. Experiment

InP NWs were grown on n-type InP (1 1 1)B substrates in the particle assisted growth mode using 80 nm monodisperse and randomly distributed gold aerosol particles in a density of  $0.5 \times 10^8 \text{ cm}^{-2}$  as seeds [14]. Trimethylindium (TMI) and, phosphine (PH<sub>3</sub>) were used as precursors with molar fractions of  $\chi_{\text{TMI}} = 18.9 \times 10^{-6}$  and  $\chi_{\text{PH}_3} = 6.25 \times 10^{-3}$ , in a total flow of 6 l/min using H<sub>2</sub> as carrier gas. The NWs were grown at 450 °C for 15 min after an annealing step at 550 °C. For non-tapered NW growth, HCl was added in a molar fraction of  $\chi_{\text{HCl}} = 20 \times 10^{-6}$ . The etch experiments **after** growth were carried out in PH<sub>3</sub>/H<sub>2</sub> to prevent rapid dissolution of the NWs by P desorption [15]. For the  $\chi_{\text{HCl}}$  dependent experiments ( $0 < \chi_{\text{HCl}} < 50.0 \times 10^{-6}$ ) the NWs were etched for 5 min at 450 °C directly **after** growth. For temperature dependent experiments, the temperature was set to  $410 \text{ °C} < T < 530 \text{ °C}$ . Upon reaching the temperature, it was stabilized for 1 min. Then *in situ* etching was carried out for 5 min using  $\chi_{\text{HCl}} = 8 \times 10^{-6}$ , after which HCl was switched off and the samples were cooled down in PH<sub>3</sub>/H<sub>2</sub>. NWs were also grown and annealed for the duration of the etch time in PH<sub>3</sub>/H<sub>2</sub> (HCl switched off) at the corresponding temperatures to deduce any influence of the annealing on NW dimensions. The NWs were characterized by scanning electron microscopy (SEM). Etch rates were obtained from the difference in length and radius of etched NWs and that of the reference NWs, evaluated using the image processing software Nanodim [16], divided by the etch time.

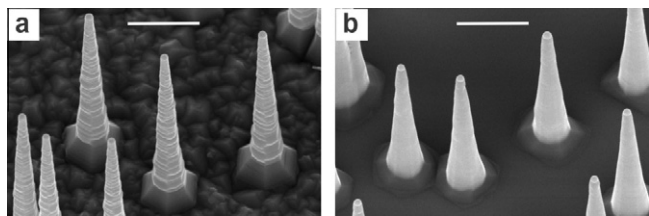
### 3. Results and discussion

Figure 1a shows reference NWs, which are about 450 nm in diameter just above the thick base. This corresponds to a radial growth rate of about 0.6 nm/s assuming a linear dependence of the shell thickness with respect to growth time [9]. Figure 1b shows the effect of etching **after** growth on the morphology of

<sup>\*</sup> Corresponding author. Fax: +46 462223637.

E-mail address: [magnus.borgstrom@ftf.lth.se](mailto:magnus.borgstrom@ftf.lth.se) (M.T. Borgström).

<sup>1</sup> On leave from Fujitsu Laboratories Limited, Japan.



**Figure 1.** SEM images of (a) reference NW (b) NW etched **after** growth for 5 min at 450 °C with  $\chi_{\text{HCL}} = 33 \times 10^{-6}$ . The scale bars are 1  $\mu\text{m}$ .

such tapered NWs. Etched NWs have a similar shape as the reference NWs with reduced length and diameter, and the NW surface is smoothened. If differences in NW side facet surface energies (hypothesis 1) were the reason for the striking perfect non-tapered growth of the NWs [6], one may argue that the tapering shell on the NW core should be removable by selective etching also **after** growth. Etching **after** growth does not develop the ‘original’ NW facets. Thus, hypothesis 1 is discarded.

In order to characterize the axial and radial etch rates without concern of geometric effects due to tapering we grew non-tapered NWs, and etched the NWs **after** growth using varied  $\chi_{\text{HCL}}$  and temperature. The  $\chi_{\text{HCL}}$  dependent results are plotted in Figure 2. For low  $\chi_{\text{HCL}}$  we observe a significant increase in NW length (740 nm) as compared to reference NWs. Some of the reaction products cause the NWs to grow, even though no TMI is supplied. In Figure 2d this is visible as a negative etch rate. For higher  $\chi_{\text{HCL}}$  we observe a seemingly linear increase in radial as well as axial etch rate with  $\chi_{\text{HCL}}$ , which indicates that the process is diffusion limited. This is in contrast to previous results on *in situ* etching of InP thin films by HCl [17,13] where InCl desorption was found to be the rate limiting step. This might find its explanation in the relatively low  $\chi_{\text{HCL}}$  used here. The etch rate is proportional to  $\chi_{\text{HCL}}$ , which suggests that the InCl desorption rate is similar to, or faster than, the rate of formation. Thus hypothesis 2 (InCl desorption limited etching) is discarded.

The etched NWs consist of a mixture of zinc blende and wurtzite segments [6]. The partly inhomogeneous radial etching visible in Figure 2b may be a consequence of etch selectivity between segments along the NW side facets. The radial etch rate (the average etch rate over the NW, excluding the top and bottom 20%) is about 0.05 nm/s at  $\chi_{\text{HCL}} = 30 \times 10^{-6}$ , a molar fraction which for etching **during** growth results in taper free NWs [6]. By comparison with the estimated radial growth rate leading to tapering (0.6 nm/s) it is clear that the etch rate of chemisorbed species is not sufficient to remove tapering occurring **during** growth. This strongly supports hypothesis 3: In adatoms sitting in a configuration with looser bonding structure and In-related decomposition species

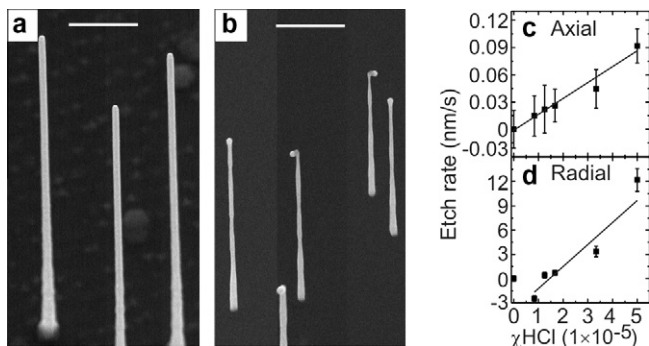


**Figure 2.** SEM images of (a) reference NW, (b) NW etched **after** growth for 5 min with  $\chi_{\text{HCL}} = 33 \times 10^{-6}$ , (c) radial etch rate **after** growth as a function of  $\chi_{\text{HCL}}$  and (d) axial etch rate **after** growth as a function of  $\chi_{\text{HCL}}$ . The lines are linear fits to the data, excluding to value at  $\chi_{\text{HCL}} = 0$  for the axial etch rate. Scale bars are 1  $\mu\text{m}$ . Error bars are standard deviations.

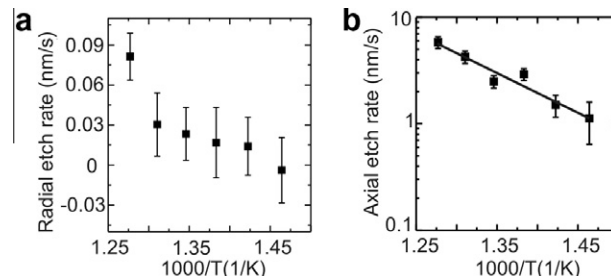


**Figure 3.** Temperature dependent experiments. (a) Linear plot of the radial etch rate as a function of inverse temperature. The  $\chi_{\text{HCL}}$  was set to  $8 \times 10^{-6}$ . (b) Semi logarithmical Arrhenius plot of the axial etch rate as a function of inverse temperature. Error bars are standard deviations.

(that exist only in etching experiments **during** growth) are more easily chlorinated than In in solid InP.

The axial etch rate is about a factor 100 more rapid than the radial etch rate with a high anisotropy as compared to other means of etching [18]. This may suggest that there is a kinetic limitation to the process. Note that unlike normal metal-assisted etching, the etchant is a gas instead of a liquid, and the metal is liquid rather than a solid.

In order to assess the kinetics of the process, temperature dependent experiments were carried out. The radial etch rate, shown in the linear plot of Figure 3a, increases with temperature but is not straightforward to analyze quantitatively due to the relatively large error bars caused by the limited NW diameter and slight variations in NW diameter. By extrapolating the data of Agnello and Gandhi [13] to 500 °C and compensating the etch rate by the difference in  $\chi_{\text{HCL}}$ , an etch rate of 0.06 nm/s is obtained, which is slightly higher than the radial etch rates we observe ( $\sim 0.02$  nm/s). Strikingly, the axial etch rate is about 100 times more rapid, even though the InP (1 1 1)B etch rate is expected to be lower than that of InP (0 0 1) [17].

The data for the axial etch rate is shown in the Arrhenius plot of Figure 3b, and suggests a kinetic barrier of 28 kJ/mol. Agnello and Gandhi found an activation barrier for *in situ* etching of InP (0 0 1) by HCl at temperatures <625 °C to be 86 kJ/mol and >625 °C to be 28 kJ/mol [13]. The rate limiting step at low temperature was related to InCl desorption. At this point we do not fully understand the low activation energy observed in our low temperature experiments. It may indicate that InCl desorption in the presence of the Au particle alloy is different from that on InP. We note however that  $\chi_{\text{HCL}}$  is relatively low [17] in our experiments and InCl desorption will not be rate limiting if occurring at the same speed or faster than InCl formation.

We speculate that the reason for the strong anisotropic etching can be found in that In dissolved in the liquid alloy particle is chlorinated more easily than chemisorbed In. Au reacts strongly with InP even down to room temperature [19] until the thermodynamically defined equilibrium phase is reached [20]. As a consequence, In depletion from the Au particle alloy via chlorination creates a driving force for dissolving In from the NW/Au-interface into the particle. We cannot rule out that HCl reacts with P at the InP (1 1 1)B-NW/Au interface to synergistically enhance the reaction.

#### 4. Summary

We conclude that the etching **after** growth is fundamentally different from **during** growth. For etching **during** growth, HCl reacts with indium based species (TMI, dimethylindium, monomethylindium, and physisorbed indium). For etching **after** growth, chemisorbed species, and In dissolved in the Au particle are involved in the reaction. The reaction products contribute to NW growth. The presence of the Au alloy particle induces a strongly

anisotropic etching with an aspect ratio of 1:100. The proposed mechanism is based on removal of indium from the liquid alloy particle by chlorination, and may be applicable also to other materials that alloy with Au and can form chlorides.

### Acknowledgements

This work was performed within the Nanometer Structure Consortium at Lund University, supported by the Swedish Research Council, the Swedish Foundation for Strategic Research, and by the EU program AMON-RA (214814). It is based on a project which was funded by E.ON AG as part of the E.ON International Research Initiative. Responsibility for the content of this publication lies with the authors.

### References

- [1] K. Hiruma, M. Yazawa, K. Haraguchi, K. Ogawa, T. Katsuyama, M. Koguchi, H. Kakibayashi, *J. Appl. Phys.* 74 (1993) 3162.
- [2] D.Y. Li, Y. Wu, R. Fan, P.D. Yang, A. Majumdar, *Appl. Phys. Lett.* 83 (2003) 3186.
- [3] M.T. Björk et al., *Nano Lett.* 2 (2002) 87.
- [4] X. Duan, Y. Huang, Y. Cui, J. Wang, C.M. Lieber, *Nature* 409 (2001) 66.
- [5] T. Mårtensson et al., *Nano Lett.* 4 (2004) 1987.
- [6] M.T. Borgström et al., *Nano. Research* 3 (2010) 264.
- [7] H.J. Joyce et al., *Nano Lett.* 9 (2009) 695.
- [8] M. Borgström, K. Deppert, L. Samuelson, W. Seifert, *J. Cryst. Growth* 260 (2004) 18.
- [9] M.A. Verheijen, G. Immink, T. deSmet, M.T. Borgström, E.P.A.M. Bakkers, *J. Am. Chem. Soc.* 128 (2006) 1353.
- [10] S.A. Dayeh, E.T. Yu, D. Wang, *Nano Lett.* 7 (2007) 2486.
- [11] K.A. Dick, K. Deppert, L. Samuelson, W. Seifert, *J. Cryst. Growth* 298 (2007) 631.
- [12] Z. Huang, N. Geyer, P. Werner, J. de Boor, U. Gösele, *Adv. Mat.* (2010) 1.
- [13] P.D. Agnello, S.K. Ghandhi, *J. Cryst. Growth* 73 (1985) 453.
- [14] M.H. Magnusson, K. Deppert, J.O. Malm, J.O. Bovin, L. Samuelson, *Nanostruct. Mat.* 12 (1999) 45.
- [15] R.S. Pennington, J.R. Jinschek, J.B. Wagner, C.B. Boothroyd, R.E. Dunin-Borkowski, *J. Phys.* 209 (2009) 012013.
- [16] Storm K., Samuelson L., (2010), submitted for publication. Available from: <[http://nanodim.kristianstorm.com/index.php?title=About\\_nanoDim](http://nanodim.kristianstorm.com/index.php?title=About_nanoDim)>.
- [17] C. Caneau, R. Bhat, M. Koza, J.R. Hayes, R. Esagui, *J. Cryst. Growth* 107 (1991) 203.
- [18] N. Sultana, W. Zhou, P. Tim, J. LaFave, D.L. MacFarlane, *J. Vac. Sci. Tech. B* 27 (2009) 2351.
- [19] A. Hiraki, S. Kim, W. Kammura, M. Iwami, *Surf. Sci.* 86 (1979) 706.
- [20] V.G. Weizer, N.S. Fatemi, *J. Appl. Phys.* 69 (1991) 8253.